Defence Science Journal, Vol. 58, No. 2, March 2008, pp. 238-247

Perforated Plates as Passive Mitigation Systems

G.S. Langdon, G.N. Nurick, V.H. Balden, and R.B. Timmis
University of Cape Town, Rondebosch 7701, South Africa

ABSTRACT

This paper presents the results of tests on fully-clamped circular plates subjected to blast loading directed down a tube. Four series of tests were performed. In one set of experiments, the blast wave was allowed to progress unhindered down the tube to impinge upon the plate, and in the other tests, perforated plates were placed in the path of the blast wave to hinder progression down the tube, disrupting the blast and absorbing some of the kinetic energy. Results of the tests indicate that the perforated plates can be used as a form of passive mitigation.

Keywords: Blast loading landmines, plastic deformation, perforated plates, passive mitigation

1. INTRODUCTION

Recently, interest has grown in the field of blast mitigation as the world events show that the risk of subversive activity appears to be increasing. In addition, there is still considerable risk to peacekeeping forces from the millions of landmines still present across the globe. Others at risk from the threat of blast loading include those working in the military, defence, transport, and process industries. Mitigation measures are often employed to attenuate the effect of blast loading upon structures. Such methods are broadly classified as either active or passive systems, depending upon the respective nature of activation of the system.

1.1 Active Mitigation Systems

Active measures are those which need to be actively deployed in response to a blast event. A schematic representation of an active mitigation system (based on a hypothetical active mitigation system for a landmine-protected vehicle) is shown in Fig. 1. Once the threat is realised (in this scenario, a landmine is detonated), the active system must first sense the threat and then activate the appropriate mitigation system. Subsequent to this, the activated system must then deploy and mitigate the effect of the threat (in this scenario, reduce the destructive effects of a landmine explosion upon the vehicle and its occupants). For the scenario of a landmine-protected vehicle, the detection and deployment process must happen within microseconds for the mitigation system to be in place to attenuate the vehicle and occupant damage. No such technology is reported within the literature than can detect the detonation and deploy within such a rapid timeframe. An example of an active blast mitigation system used in practice would be the water deluge systems used on UK offshore oil and gas platforms. The system does not wait for detonation. Upon detection of a gas leak, water droplets are released into the affected area to mitigate the effect of the potential gas explosion that may ensue[1].

Received 31 October 2007

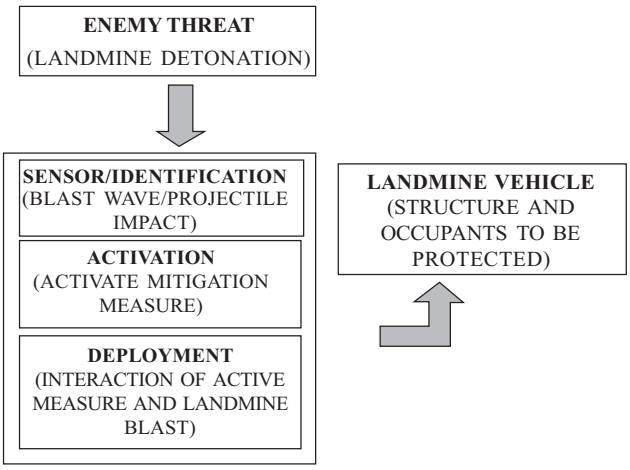

Figure 1. Schematic representation of an active mitigation system.

1.2 Passive Mitigation Systems

Passive mitigation systems are those that are embedded within the structural design and require no trigger mechanisms for activation. For most blast scenarios, such systems are usually preferred as they do not rely upon detection and deployment mechanisms, but are always activated. Broadly speaking, there are four approaches to passive mitigation, although some systems use more than one approach:

- *Impedance mismatching*: For example: (a) placing a water-filled cavity between the incident blast wave and the structure to be protected, and (b) using elastomer layers impregnated with air-filled microspheres[2].
- *Sacrificial cladding*: Cladding layers used to absorb the energy through plastic deformation, while limiting the force transfer through it to the stress-strain characteristic of the material. An example of such a system would be the use of metal foams as sacrificial cladding layers[3]. The employment of plastically deforming (metal) plates[4] and sandwich structures[5-9] to absorb energy for impact and blast loading applications are reported widely in the literature.
- *Blast deflection*: These systems redirect the blast wave away from the structure to be protected. This is an established technology in old current generation landmine-protected vehicles, such as the Casspir[10] and the ADI Bushmaster[11], which have V-shaped hulls to deflect the blast away from the hull.
- *Blast and shockwave disruption*: These systems employ some object between the blast wave source and the target to disrupt the path of the blast wave. Such systems could include granular filters[12], or geometric obstacles such as barriers[13] and baffles[14]. For example, Berger[13], *et al.* explored the use of concrete barriers in tunnels to mitigate shock loading, both experimentally and numerically (using a hydrodynamic code).

In this study, perforated plates in a passive mitigation system are used. There is no information available in the open literature about the effect of perforated plates on blast wave propagation, although perforated plates have been used in shock tubes to disrupt shock waves by Medvedev[15] and Chaoa[16], *et al.*

Different perforated plate designs were used by Medvedev[15], with the number of holes in the plate, the sizes of these holes, and the distance between holes being used as design variables. A blockage ratio (BR) parameter was defined, equal to the ratio of the area of solid material to perforated material as defined in following equation

$$BR = 1 - \frac{N \times d^2}{D^2} \quad (1)$$

where N is the total number of the holes, d is the hole dia, and D is the disc dia.

Medvedev[15] examined the influence of various BR values and found that increasing BR (for example by using less holes or smaller dia holes) resulted in the significant attenuation of the shockwave velocity[15]. One of the plate configurations examined[15] is shown in Fig. 2.

Chaoa[16], *et al.* used the ratio of hole spacing to hole dia (known as the *l/d* ratio) as a parameter in their testing of detonation quenching. Although in this instance, the ratio was maintained at a constant value of 0.5, a variation of this ratio can effectively be seen as a variation of a blockage ratio. This is because both the BR and the *l/d* ratio are dependant

Figure 2. Typical perforated plate design[15].

on hole dia, and if the spacing between holes is increased without increasing the hole dia, the ratio of solid material to perforated material increases.

This study reports the results of an experimental investigation that employs perforated plates located between the blast-loading source and the protected object (in this case, a fully-clamped deformable target plate).

2. EXPERIMENTAL PROCEDURE

2.1 Perforated Plate Design

A perforated plate deign was formulated, as shown in Fig. 2. Only one plate geometry was considered in this preliminary study, with six equi-spaced holes arranged around a larger dia inner hole. The area of the plate exposed to the blast wave is shown as a shaded region in Fig. 3. The other holes shown in Fig. 3(a) are for clamping. The blockage ratio of the chosen design is 0.87 and the ratio of hole spacing to hole dia (*l*/*d*) is one-forth.

2.2 Experimental Method

A photograph of the experimental arrangement is shown in Fig. 3(b). Three tubes, each 150 mm long with a 106 mm internal dia, were employed in series. At the front end of the first (front) tube, a disc of PE4 explosive was located. A small leader of explosive was used to attach an electrical detonator to the centre of the disc. Once detonated, a blast wave propagated down the tube towards the target plate (considered to be a worst case scenario: in the practical case, the blast wave would propagate spherically). This is similar to the method employed by Jacob[17], *et al*. in a recent study which examined the influence of stand-off distance (SOD) on plate deformation. In the experiments reported by Jacob[17], the SOD was varied from 13 mm to 300 mm using different length tubes down which the blast loading was directed. Plate responses varied from that considered typical for locally blast-loaded plates (at small SODs, typically less than the plate radius) to those typically observed for

(a)

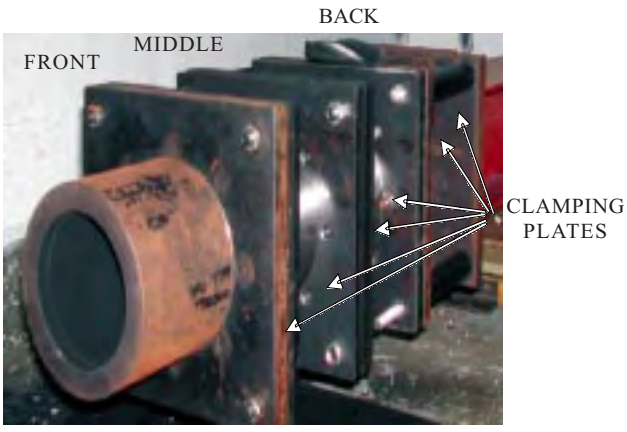

(b)

Figure 3. Experimental details: (a) perforated plate design (hatched area shows area exposed to the blast wave) and (b) ballistic pendulum arrangement.

uniformly loaded plates (at greater SODs, typically over one plate dia). Jacob[17], *et al*. also observed that the displacement for a given charge mass decreased with increasing SOD until a minimum was observed at SOD of 250 mm. Increase of the SOD beyond 250 mm (to 300 mm) did not decrease the measured plate displacement.

The experimental layout is shown schematically in Fig. 4. A 1.6 mm thick deformable mild steel plate was clamped at the back-end of the third (back) tube, a total distance of 454 mm from the front-end of the first tube. This deformable plate is known herein as the target plate. After each test, the permanent mid-point displacement of the target plate was measured. Average permanent displacement of perforated plates (inner annulus) was also measured post-test. Impulse was determined from the swing of the pendulum[18].

2.3 Test Matrix

All sets of experiments had a 1.6 mm thick target plate at the rear that deformed according to the spatial and temporal characteristics of the incident pressure pulse. Depending upon the test configuration, either 2 mm thick perforated plates or 2 mm thick spacer plates were clamped between the front (1st) and middle (2nd) tubes (position F), and between the middle (2nd) and back (3rd) tubes (position M). The test matrix is given in Table 1. The tubes were then clamped onto the ballistic pendulum to enable measurement of the impulse, as shown in Figs 3 and 4. Four sets of experiments were performed, with perforated plates in different positions:

Table 1. Test matrix

Position of plate in tube	Front/middle interface (F)	Middle/back interface (M)	Target plate
Set identifier			
[—B]	No	No	Deformable
[F–B]	Perforated	No	Deformable
[-MB]	No	Perforated	Deformable
[FMB]	Perforated	Perforated	Deformable

- Set 1 (—B): These were baseline tests at a SOD of 454 mm, and contained no perforated plates.
- Set 2 (F-B): These tests employed a perforated plate between the front and middle tubes, a distance of 150 mm from the explosive detonation.
- Set 3 (-MB): These tests were performed with a perforated plate between the middle and back tubes, a distance of 302 mm away from the explosive, but no plate in the front position.
- Set 4 (FMB): These tests employed perforated plates at both positions, between the front and middle tubes, and also between the middle and back tubes.

A minimum of five tests were performed for each configuration.

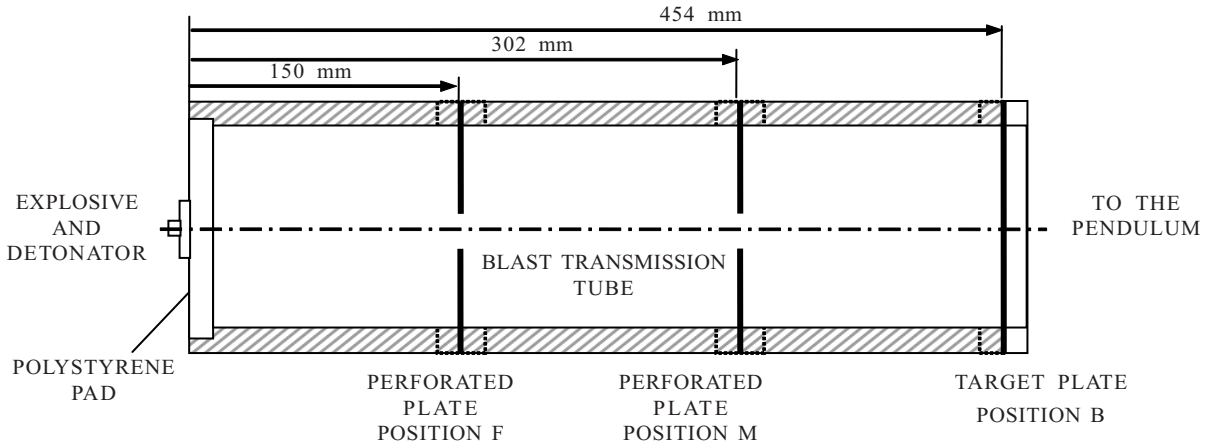

Figure 4. Experimental layout.

3. RESULTS AND OBSERVATIONS

Results from tensile tests showed that the material used to manufacture the target plates and the perforated plates had static (corrected using the Cowper-Symonds relation with D = 40.4 s^{-1}, q = 5) yield stresses of 275 MPa and 243 MPa, respectively. Mean average percentage elongation was measured to 42 per cent and 39 per cent, respectively for the two batches of steel.

The results from the blast loading experiments are given in Table 2. A graph of back plate deflection versus impulse is shown in Fig. 5. In agreement with observations by Nurick[17-19], *et al.* mid-point deflection is observed to increase linearly with increasing impulse within a test configuration. The results also show that the deflection of the back plate is reduced by the insertion of perforated plates in the path of the blast wave. Deflection of the target plates was reduced by 65-75 per cent with the insertion of one perforated plate, and 90-95 per cent with the insertion of two perforated plates. From photographs of the perforated plates shown in Fig. 6 it is evident that considerable damage is sustained, absorbing significant amounts of strain energy. Two sets of tests were performed with one perforated plate used. One set had a perforated plate in position M, and the other had a perforated plate in position F. It is observed from Fig. 5 that there is a slight difference in the target plate deflection between the tests with the perforated plate in the F and M positions. The mid-point deflections of the target plates with the perforated plate closer to the target (that is, position M) were higher than those with the perforated plate further way (position F).

Further testing is required to ascertain the relative contributions of: (a) the disruption of the blast wave propagation, and (b) the energy absorption of the perforated plates (through deformation and tearing). The disruption mechanism in particular not well understood.

4. NONDIMENSIONAL ANALYSIS

In 1972, Johnson[20] proposed a damage number in nondimensional form for impulsively-loaded plates. Nurick and Martin[21] introduced modifications to Johnson's damage number that included geometry and loading conditions. This parameter has become known as nondimensional impulse and is shown for monolithic circular plates as

$$\phi_c = \psi\lambda\zeta = \overbrace{\left[\frac{I^2}{H^2\rho\sigma_d}\left(\frac{A_0}{A}\right)^2\right]^{1/2}}^{\text{GEOMETRIC DAMAGE NUMBER}} \times \underbrace{\frac{R}{H}}_{\text{ASPECT RATIO}} \times \underbrace{\left(1+\ln\left(R/R_0\right)\right)}_{\text{LOADING PARAMETER}} = \frac{I\left(1+\ln\left(R/R_0\right)\right)}{\pi RH^2\left(\rho\sigma_0\right)^{1/2}} \quad (2)$$

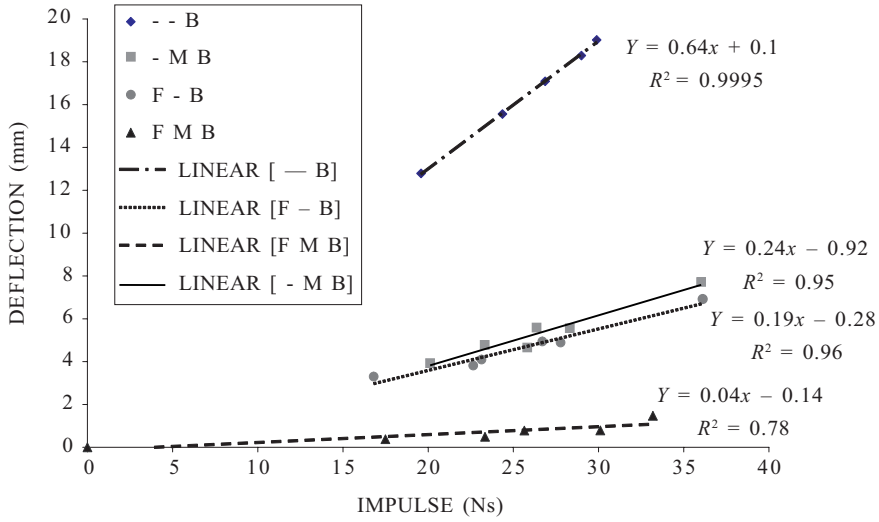

Figure 5. Deflection of the back plate versus impulse for the perforated plate tests.

Table 2. Results from blast loading experiments

Panel type	Panel name	Charge mass* (g)	Impulse(Ns)	Permanent deflection(mm)		
				Deformable target plate	Perforated plate F	Perforated plate M
Baseline tests (no perforated plates)[—B]	1.6	9	19.6	12.8	-	-
	1.3	11	24.4	15.6	-	-
	1.5	12.5	26.9	17.1	-	-
	1.4	14.5	29.0	18.3	-	-
	1.2	16	29.9	19.0	-	-
	1.1	21	31.0	-	-	-
Perforated plate in front position[F-B]	2.6	9	16.8	3.3	13.3	-
	2.2	11	22.7	3.8	14.5	-
	2.5	12.5	23.1	4.1	16.5	-
	2.4	14.5	26.7	4.9	19.0	-
	2.1	16	27.8	4.9	20.8	-
	2.3	21	36.1	6.9	Torn	-
Perforated plate in middle position[-MB]	3.6	9	20.1	3.9	-	10.9
	3.2	11	23.3	4.8	-	12.6
	3.5	12.5	25.8	4.7	-	14.3
	3.4	14.5	26.4	5.6	-	15.9
	3.1	16	28.3	5.6	-	16.6
	3.3	21	36.0	7.7	-	20.6
Perforated plate in both positions[FMB]	4.6	9	17.5	0.3	13.3	1.7
	4.1	11	-	0	14.6	2.0
	4.5	12.5	23.3	0.5	16.2	2.7
	4.4	14.5	25.6	0.8	17.9	3.5
	4.2	16	30.1	0.8	20.4	3.6
	4.3	21	33.2	1.5	Torn	4.3

* Charge masses do not include the 1 g leader of explosive between the PE4 disc and the electrical detonator.

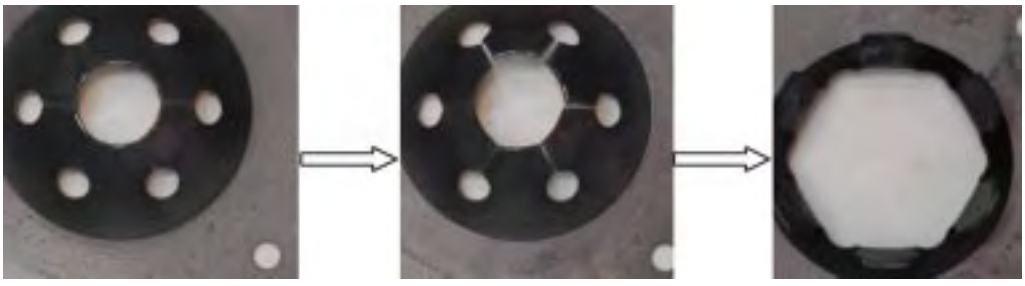

a **b** **c**

Figure 6. Perforated plates, test configuration [FMB] with charge masses (do not including 1.0 g leader): (a) 13.5 g, (b) 15.0 g, and (c) 20 g.

where ϕ_c is the nondimensional impulse; λ is the aspect ratio; ρ is density; σ_d is the dynamic flow stress; σ_0 is the static yield stress; ψ is the geometrical damage number; ζ is the loading parameter; A_0 is the area over which impulse is imparted; A is the plate area; H is the plate thickness; I is the impulse; R is the plate radius; and R_0 is the load radius.

Since $\left(\frac{A_0}{A}\right) = 1$ for uniformly loaded circular plates, the $\psi\lambda\zeta$ product reduces to the right hand side of Eqn (2) when the static yield stress is substituted for the dynamic flow stress. This is a common substitution as it is difficult to estimate the dynamic flow stress as the strain rate in the plate is unknown (and variable throughout the deformation process). Jacob[17], *et al.* proposed a modification to the loading parameter ζ to incorporate the influence of SOD into the nondimensional impulse, as shown in Eqn (2) for monolithic circular plates. Nondimensional displacement – nondimensional impulse charts have been plotted, and a linear relationship was observed that is described by the following equations

$$\phi_{cS} = \frac{I\left(1 + \ln\left(R/R_0\right)\right)}{\pi RH^2\left(1 + \ln\left(S/R_0\right)\right)\left(\rho\sigma_0\right)^{1/2}} \text{ for } R_0 \le S \quad (3)$$

$$\frac{\delta}{H} = 0.425\phi_C \quad (4)$$

where δ is mid-point permanent displacement of the plate.

The impulse required to deform the target plate at the rear of the experimental assembly can be found by combining Eqns (3) and (4), as shown in Eqn (5). Jacob[17], *et al.* observed that, as SOD increased beyond 250 mm, there was no change in displacement for a particular experimental configuration. To account for the effect of greater SODs (that is $S > 0.25$ m), S in Eqn (3) is fixed at a maximum of 250 mm. The current tests employed the same charge dia and tube radius used by Jacob[17], *et al.* but at a greater SOD (0.454 m). For these tests, S was fixed at 0.25 m to account for SOD in the loading parameter. Equation (5) was used to determine the impulse required to deform the target plate by the amount measured post-test. A graph of the empirical predictions of impulse from Eqn (5) versus the measured impulse (calculated from the swing of the pendulum) is shown in Fig. 7 for the experiments without a perforated plate. It can be observed that there is good agreement when a value S of 0.25 m was used, hence for test series 1, the experimental data agrees with that obtained by Jacob[17], *et al*. This gives confidence that the empirical equation can provide a good prediction of permanent displacement for this experimental configuration.

$$I_{TP} = \frac{\delta\pi RH\left(\rho\sigma_0\right)^{1/2}\left(1 + \ln\left(S/R_0\right)\right)}{0.425\left(1 + \ln\left(R/R_0\right)\right)} \quad (5)$$

where $S = 0.25$ m in accordance with the observations of Jacob[17], *et al*.

Next, it was assumed that the loading of the target plate is still uniformly distributed (and impulsive) when a perforated plate is inserted into either of the F or M locations. This assumption seems to be a reasonable working hypothesis given that the plate response looks typical of a uniformly loaded plate. Equation (5) is used to calculate the impulse required by the target plate to deform to the measured mid-point deflection value (I_{TP}). A residual impulse was calculated by subtracting the target plate impulse I_{TP} from the total measured pendulum impulse (I), as shown in Eqn (6). The residual impulse (I_R) was used to calculate a nondimensional impulse at the perforated plate SOD for the test series (F-B) and (-MB).

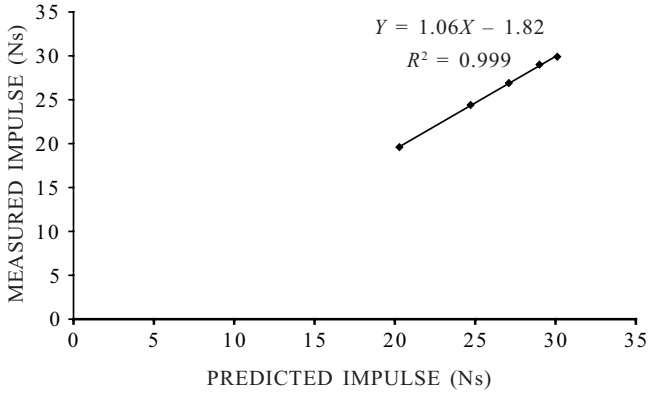

Figure 7. Empirically predicted impulse and experiment for test series 1 (no perforated plates, SOD 454 mm).

$$I - I_{TP} = I_R \tag{6}$$

Since the perforated plates contained several holes, a modification to the aspect ratio λ was introduced, following Cloete[22], *et al*. Cloete[22], *et al.* derived, for blast-loaded annular plates, similar equations to Nurick and Martin[21] using an energy analysis with an assumed mode shape to calculate the strain energy. These are shown, in slightly modified form, in Eqns (7) and (8).

$$\phi_C = \frac{I\left[R - R_i\right]}{\pi\left(R^2 - R_i^{\,2}\right)H^2\left(\rho\sigma_0\right)^{1/2}} \tag{7}$$

$$\frac{\delta}{H} = \frac{1}{\sqrt{\alpha}}\phi_C \tag{8}$$

There were three main differences:

(1) The inclusion of an α parameter in Eqn (8) which accounted for strain rate, not to be confused with the α symbol used for Johnson's[20] damage number.

(2) The absence of the load parameter, as Cloete[22], *et al*. reported results from experiments that did not employ a tube arrangement and a large SOD. Cloete[22], *et al*. obtained an approximately uniform loading distribution by using a ring-shaped charge at a SOD of 30 mm.

(3) The inclusion of an $(R_o - R_i)$ term in the numerator (instead of R).

Herein, λ is modified as $(R - R_i)/H$, to account for the central hole in the perforated plate. The other six holes are not accounted for in the λ parameter, only in the plate area calculation. Residual nondimensional impulse was calculated according to the following equation:

$$\phi_{cS_{RESIDUAL}} = \frac{I_R\left[R - R_i\right]\left(1 + \ln\left(R/R_0\right)\right)}{\pi\left(R^2 - R_i^2 - 6R_h^{\,2}\right)H^2\left(1 + \ln\left(S/R_0\right)\right)\left(\rho\sigma_0\right)^{1/2}} \tag{9}$$

where R_i is the radius of the central perforation; R_h is the radius of the six off-centre perforations, and I_R is the residual impulse. The stand-off distance S was the distance from the charge to the perforated plate in the appropriate position. For position F, S = 0.15 m; for position M, S was idealised to 0.25 m.

A graph of normalised perforated plate displacement versus this residual nondimensional impulse is shown in Fig. 8 for configurations (F-B) and (-MB). It can be noted that while the intercepts of the trend-lines through the data vary, the gradients of the trend-line equations are similar, both 0.29±0.01.

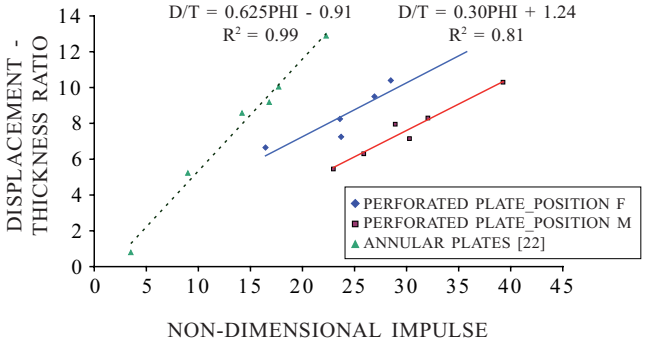

Figure 8. Normalised perforated plate displacement versus nondimensional residual impulse for test configurations (F-B) and (-MB).

For comparison, experimental results on blast-loaded annular plates from Cloete[22], *et al*. have been put into the same nondimensional form and plotted with the data in Fig. 8. The trend-line for the annular plates mentioned by Cloete[22], *et al.* had a gradient of 0.62, approximately double that of the perforated plates reported herein. The nondimensional analysis accounts for parameters such as plate thickness, dia and yield stress, but does not account for the geometry of the perforations (except in terms of the plate mass, and distance from displacement edge to boundary edge). The plates tested by Cloete[22], *et al*. were of 100 mm dia with a 22 mm dia central hole, giving a BR of 0.95. This is higher than the BR of the perforated plates examined herein (0.87).

5. CONCLUSIONS AND FUTURE RESEARCH

This study shows, by reporting the results of an experimental study, that the placing perforated plates in the path of a blast wave travelling down a tube

will mitigate the effect of the blast loading on a structure when the plates are spaced well apart from the target. Deflection of the deformable target plates were reduced by 65-75 per cent with the insertion of one perforated plate, and 90-95 per cent with the insertion of two perforated plates. The influence of perforated plate position in the tube has not been addressed. This preliminary study opens up many questions regarding the mechanism of mitigation and the influence of the perforated plate design. However, the concept for blast mitigation appears promising and further research is currently underway.

ACKNOWLEDGEMENTS

The authors wish to acknowledge Mr G. Newins, Mrs P. Park-Ross, Mr I.B. Rossiter, Mr R. W. Timmis, and Mr S.B. Nurick for their assistance in the workshop and with the experiments. Mr I.B. Rossiter and Mr T.J. Cloete are also thanked for their discussions with regard to the nondimensional analysis.

REFERENCES

1. Pritchard, D. Review of explosion mitigation measures for platform legs. Health and Safety Laboratory Report No. HSL/2006/64, 2006. http://213.212.77.20/research/hsl_pdf/2006/hsl0664.pdf (Accessed Sept 2007).

2. Composite floor armour for military tanks and the like. US Patent No. USP 4404889.

3. Hanssen, A.G.; Enstock, L. & Langseth, M. Close range blast loading of aluminium foam panels. *Int. J. Impact Engg.,* 2002, **27**, 593-18.

4. Guruprasad, S. & Mukherjee, A. Layered sacrificial claddings under blast loading: Part II – Experimental studies. *Int. J. Impact Engg.*, 2000, **24**, 975-84.

5. Wei, Z.; Dharmasena, K.P.; Wadley, H.N.G. & Evans, A.G. Analysis and interpretation of a test for characterising the response of sandwich panels to water blast. *Int. J. Impact Engg.*, 2007, **34**, 1602-618.

6. Vaziri, A. & Hutchinson, J.W. Metal sandwich plates subject to intense air shocks. *Int. J. Solids Struct.*, 2007, **44**, 2021-035.

7. Yu, J.L.; Wang, X.; Wei, Z.G. & Wang, E.H. Deformation and failure mechanism of dynamically-loaded sandwich beams with aluminium foam core. *Int. J. Impact Engg.*, 2003, **28**, 331-47.

8. Theobald, M.D. & Nurick, G.N. Numerical investigation of the response of sandwich-type panels using thin-walled tubes to blast loading. *Int. J. Impact Engg.*, 2007, **34**, 134-56.

9. Liang, C.C.; Yang, M.F. & Wu, P.W. Optimum design of metallic corrugated core sandwich panels subjected to blast loads. *Ocean Engineering*, 2001, **28**, 825-61.

10. Stiff, P. Taming the landmine, Galago, 1986.

11. Thanes Australia. Bushmaster, outstanding crew protection and survivability. Promotional literature, 2006.

12. Britan, A.; Ben-Dor, G.; Igra, O. & Shapiro, H. Development of a general approach for predicting the pressure fields of unsteady gas flows through granular media. *J. Appli. Phys.*, 2006, **99**(93519), 1-12.

13. Berger, S.; Sadot, O.; Melamud, G.; Anteby, I.; Kiviti, Y.; Britan, A. & Ben-Dor, G. Attenuation of shock waves by barriers in tunnels and corridor type structures. *In* Proceedings of the 2nd International Conference on Design and Analysis of Protective Structures, Singapore, 2006.

14. Smith, P.D.; Vismeg, P.; Teo, L.C. & Tingey, L. Blast wave transmission along rough-walled tunnels. *Int. J. Impact Engg.,* 1998, **21**(6), 419-32.

15. Medvedev, S.P.; Khomik, S.V. & Olivier, H. Experimental setup, measurement technique and test conditions for explosions with active/passive additives. *EXPRO* Deliverable Report D5, Contract EVG1-CT-2001-00042, March 2003.

16. Chaoa, J.; Otsukab, T. & Leea, J.H.S. An experimental investigation of the onset of detonation. *Proc. Comb. Ins.,* 2005, **30**(2), 1889-897.

17. Jacob, N.; Nurick, G.N. & Langdon, G.S. The effect of stand-off distance on the failure of fully clamped circular mild steel plates subjected to blast loads. *Engineering Structures*, 2007, **29**, 2723-736.

18. Nurick, G.N. & Radford, A.M. Deformation and tearing of clamped circular plates subjected to localised central blast loads. *In* Recent developments in computational and applied mechanics: A volume in honour of John B. Martin. International Centre for Numerical Methods in Engineering (CIMNE), Barcelona, Spain, 1997. pp. 276-301.

19. Teeling-Smith, R.G. & Nurick, G.N. The deformation and tearing of circular plates subjected to impulsive loads. *Int. J. Impact Engg.*, 1991**, 11**(1), 77-92.

20. Johnson, W. Impact strength of materials, Edward Arnold Publ., 1972.

21. Nurick, G.N. & Martin, J.B. Deformation of thin plates subjected to impulsive loading–a review, Part II–Experimental studies. *Int. J. Impact Engg.*, 1989, **8**(2), 170-86.

22. Cloete, T.J.; Nurick, G.N. & Palmer, R.N. The deformation and shear failure of peripherally clamped centrally supported blast loaded circular plates. *Int. J. Impact Engg.*, 2005**, 32**, 92-117.

Contributors

Dr Genevieve Langdon received her PhD (Mech Engg) from the University of Liverpool in 2003. Presently, she is working as Senior Lecturer at the University of Cape Town, USA, and is part of the Blast Impact and Survivability Research Unit (BISRU). Her research interests include the response of structures to blast loading, particularly emphasising passive mitigation and non-traditional materials for blast protection. She has co-authored over 35 publications in refereed journals and conference proceedings.

Prof G.N. Nurick received his PhD (Mech Engg) from the University of Cape Town, USA, in 1987. He is a professor in the Dept of Mechanical Engineering at the University of Cape Town, and concurrently is the Director, BISRU. His research interests range from detonics, structural response from impact and blast events, material characterisation and human-impact response. He has authored and co-authored over 150 publications in refereed journals, conference proceedings, invited presentations, book chapters, and reports.

Mr V.H. Balden obtained his MSc (Mech Engg) from the University of Cape Town, USA. He is working as Research Officer at the BISRU and a consultant for industry. His research interests are in the high-strain rate response of structures and materials, and finite element simulations.

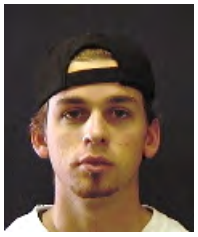

Mr Robert Timmis received his BSc (Mech Engg) from the University of Cape Town, USA, in 2006. He is currently working at the nuclear power industry.